

# Versatile transporter apparatus for experiments with optically trapped Bose-Einstein condensates

Daniel Pertot, Daniel Greif<sup>†</sup>, Stephan Albert<sup>‡</sup>,  
Bryce Gadway, and Dominik Schneble

Department of Physics and Astronomy, Stony Brook University,  
Stony Brook, NY 11794, U.S.A.

E-mail: dpertot@ic.sunysb.edu

**Abstract.** We describe a versatile and simple scheme for producing magnetically and optically-trapped  $^{87}\text{Rb}$  Bose-Einstein condensates, based on a moving-coil transporter apparatus. The apparatus features a TOP trap that incorporates the movable quadrupole coils used for magneto-optical trapping and long-distance magnetic transport of atomic clouds. As a stand-alone device, this trap allows for the stable production of condensates containing up to one million atoms. In combination with an optical dipole trap, the TOP trap acts as a funnel for efficient loading, after which the quadrupole coils can be retracted, thereby maximizing optical access. The robustness of this scheme is illustrated by realizing the superfluid-to-Mott insulator transition in a three-dimensional optical lattice.

PACS numbers: 67.85.-d, 37.10.Gh, 67.85.Hj

<sup>†</sup> Present address: Institute for Quantum Electronics, ETH Zürich, 8093 Zürich, Switzerland.

<sup>‡</sup> Present address: Physik Department, Technische Universität München, 85748 Garching, Germany.

## 1. Introduction

Techniques for the optical trapping and manipulation of Bose-Einstein condensates have enabled experiments on a broad range of topics including Feshbach resonances [1], spinor condensates [2], and many-body effects in optical lattices [3]. Moreover, all-optical schemes [4] have eliminated the need for magnetic trapping in evaporative cooling applications. Nevertheless, the use of magnetic traps remains attractive due to their large volume, depth and passive stability. Major recent developments include the advent of miniaturized chip-based magnetic traps [5] and the realization of transporter apparatus designs [6–9] in which the main chamber used for laser cooling is spatially separated from the science cell in which experiments with the condensate are performed.

Two generic types of transporter apparatus can be distinguished. In one type, an evaporatively cooled cloud in or near the quantum degenerate regime is first produced in the main chamber and subsequently delivered into the science cell using an optical tweezer [8, 9]. In the second type, a laser-cooled, magnetically trapped cloud is first moved into the science cell, before evaporation is performed. Here, the transport is achieved by either using a chain of overlapping stationary coil pairs [6], or by mechanically displacing a single, movable pair of coils [7]. Transporter machines have become increasingly popular, and both the optical and magnetic types are now in use by a number of groups.

In comparing the two apparatus types, a certain complementarity can be noticed. The optical tweezer design allows for nearly unobstructed optical access in the science cell, but it requires the ability to perform evaporative cooling already in the main chamber, thus imposing stringent conditions on the vacuum and complicating apparatus design. In contrast, magnetic transporters only require a simple vapor cell for laser cooling, but the presence of a permanent magnetic coil assembly for evaporation restricts optical access in the science cell.

In this paper, we present a novel implementation of a magnetic-coil transporter apparatus, based on moving coils, that shares the advantages of the optical tweezer scheme and also minimizes the overall design complexity: by adding a homogeneous rotating bias field to that of the movable coil pair, a stable trap of the TOP type [10], well-suited for condensate production, is formed in the science cell. Since the same quadrupole coil pair is used for magneto-optical trapping, transport, and evaporation, the TOP trap can thus be operated as a “retractable funnel” to load an optical trap, resulting in almost unobstructed optical access.

Hybrid traps, realized by the addition of either a blue [11, 12] or red [13] detuned laser beam to the quadrupole potential, could present an alternative to the solution presented here in the context of a moving-coil magnetic transporter. However, retaining the ability to produce condensates in an alignment-free configuration seems advantageous for stable day-to-day operation. Also, we are able to efficiently load condensates into optical traps without incurring the need for high beam intensities.

This paper is organized as follows: Section II gives an overview of the experimental setup, before the general features and technical implementation of the TOP trap are discussed in section III. Section IV characterizes the performance of the trap for condensate production, and section V illustrates its use in conjunction with optical trapping applications.

## 2. Overview of experimental setup

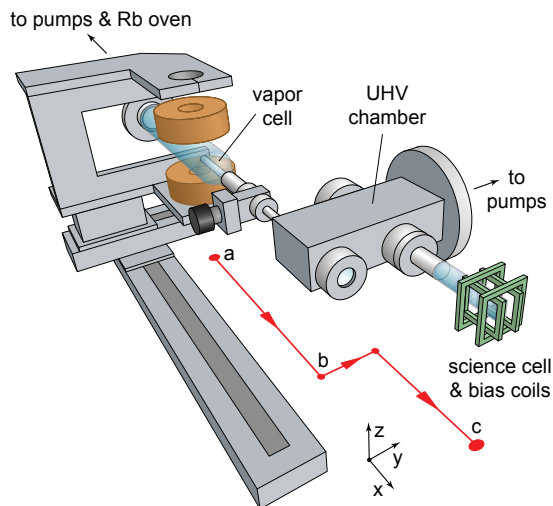


**Figure 1.** Transporter apparatus. The vapor cell is made from a 5.7 cm-diameter Pyrex tube and is connected through valves with an ion pump and a rubidium reservoir (not shown), maintaining a rubidium background pressure of several  $10^{-9}$  torr. A 28 cm-long tube of 1 cm inner diameter connects the vapor cell to the UHV chamber and the attached science cell, which are pumped down to less than  $10^{-11}$  torr by an ion pump in combination with a titanium sublimation pump (not shown). The quadrupole coils (shown in MOT position ‘a’) are mounted on an aluminum holder (sliced to reduce eddy currents) that sits on two orthogonally stacked translation stages (Parker Daedal 404XR). The kink in the translation path protects the science cell from fast ballistic atoms escaping from the vapor cell, and it enhances optical access to the condensate along the  $x$ -axis. A small gate valve located midway in the pumping tube allows to completely disconnect the two vacuum regions for servicing.

Our moving-coil transporter apparatus is illustrated in figure 1. A cylindrical glass vapor cell is connected to a UHV chamber with an attached small quartz glass science cell (cf. also figure 2) through a differential pumping tube. In the vapor cell, we collect up to  $1.5 \times 10^{10}$  atoms in a standard six-beam  $^{87}\text{Rb}$  MOT, making use of light induced atom desorption (LIAD) [14–16] to temporarily enhance the loading rate. After an 8 ms molasses phase that lowers the temperature to about  $25 \mu\text{K}$ , the atoms are optically pumped to the  $|F = 1, m_F = -1\rangle$  hyperfine ground state, and subsequently caught in a magnetic quadrupole trap using the same coil pair as for the MOT at an axial field gradient of  $100 \text{ G/cm}$ , yielding  $2.2 \times 10^9$  trapped atoms at  $150 \mu\text{K}$ .

The quadrupole coils are mounted on a mechanical translation stage assembly, which is used to move the magnetically trapped cloud into the science cell. This is done as quickly as possible ( $a = 4.5 \text{ m/s}^2$ ,  $v_{\text{max}} = 0.94 \text{ m/s}$ ) in order to minimize losses due to collisions with background gas atoms in the vapor cell. The quadrupole trap is simultaneously compressed to its final axial field gradient of  $B'_z = 350 \text{ G/cm}$  within 150 ms before the cloud reaches the pumping tube. This adiabatically heats up the cloud to  $450 \mu\text{K}$ . We have confirmed that non-adiabatic heating during the motion amounts to less than  $10 \mu\text{K}$ .

Once the cloud reaches the UHV chamber ‘b’, where the measured lifetime exceeds 150 s, the transporter slows down and proceeds along a kinked path ( $a = 0.5$  m/s<sup>2</sup>,  $v_{\max} = 0.18$  m/s). After a total travel time of 3 s and a covered distance of 66 cm, about  $1.6 \times 10^9$  atoms, or 75% of the atoms initially caught, arrive in the science cell ‘c’, where they are evaporatively cooled as discussed in section 4. We attribute the loss of atoms during the motion to background gas collisions while moving out of the vapor cell, and to a possible shaving off of hot atoms on the walls of the differential pumping tube.

### 3. Moving-coil TOP trap

Instead of producing the condensate in a separate Ioffe-Pritchard trap, as generally found in transporter apparatus based on [7], we use the movable quadrupole coils as an integral part of the final magnetic trap. This could be done, in principle, by realizing either a TOP trap [10] or a QUIC trap [17]. For the latter, however, the trap bottom depends on the delicate cancelation of the much larger fields of the quadrupole coils and the Ioffe coil, making the trap very sensitive to fluctuations of their relative positions.

For a TOP trap, the trap bottom is solely determined by the magnitude  $B_0$  of the rotating bias field. It is therefore inherently insensitive to the relative positioning of the coils provided that the bias field is sufficiently homogeneous. With the bias field rotating in the  $xy$ -plane, the time-averaged magnetic potential at the center of the trap is given by

$$V(\rho, z) = \mu B_0 + \frac{1}{2} m \omega_{\perp}^2 \rho^2 + \frac{1}{2} m \omega_z^2 z^2 \quad (\rho, z \ll \rho_0). \quad (1)$$

Here,  $m$  denotes the atomic mass,  $\mu$  the magnetic moment, and  $\rho_0 = B_0/B'_{\perp}$  is the radius of the “circle-of-death” on which the field-zero is moving [10], where  $B'_{\perp} = B'_z/2$  is the radial quadrupole field gradient. The radial and axial trap frequencies are  $\omega_{\perp} = B'_{\perp}(\mu/2mB_0)^{1/2}$  and  $\omega_z = \sqrt{8}\omega_{\perp}$ , respectively. A further advantage of a TOP trap is that magnetic field fluctuations on time scales much slower than the trap frequencies do not affect the trap bottom, unlike for dc magnetic traps. Our “moving-coil TOP trap” (McTOP) is formed by combining the movable quadrupole coils with stationary bias-field coils at the science cell, as illustrated in figure 2. We note that a similar strategy has been used in [18] in conjunction with a magnetic waveguide.

Each of the water-cooled quadrupole coils consists of 33 turns of 1/4 inch-diameter coated hollow copper tubing. At a current of 425 A, the quadrupole coils ( $L = 90$   $\mu$ H) produce an axial field gradient of  $B'_z = 350$  G/cm, which can be switched off completely within less than 1 ms using an IGBT. The bias-field coils are designed to provide a maximally homogeneous bias field, while minimally obstructing the optical access to the trap center for the given science cell geometry, as shown in figure 2. The outer  $B_x$  (inner  $B_y$ ) coils each consist of 25 (20) turns of 24 AWG (0.5 mm-diameter) magnet wire and are wound onto a stiff fiberglass holder structure. Each coil pair produces a field of 7.5 G/A at the center of the trap with a simulated field inhomogeneity of less than  $\pm 3 \times 10^{-4}$  within a distance of 1 mm from the center. The air-cooled coils can thermally withstand ac currents of 8 A amplitude for the duration of the evaporation, corresponding to a 60 G bias field and a circle-of-death radius  $\rho_0 = 3$  mm at the maximum quadrupole field.

To drive the bias-field coils, we use an 800 W audio power amplifier (PA). For each coil pair, the impedance at the 10 kHz driving frequency is minimized down to

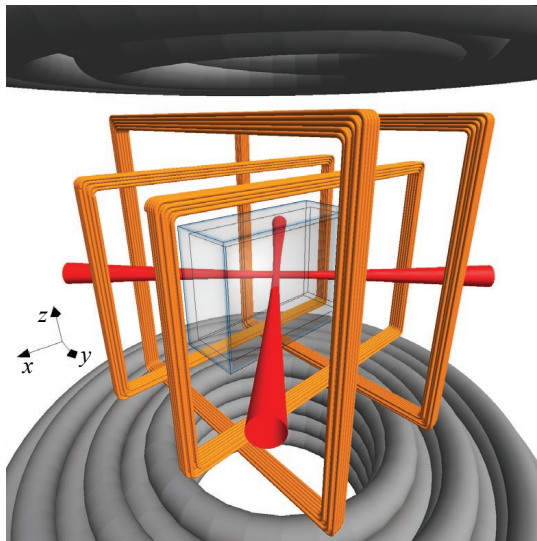


**Figure 2.** Moving-coil TOP trap configuration (McTOP) around the science cell. The rectangular bias-field coils have dimensions of  $56\text{ mm}\times 37\text{ mm}$  (inner coils) and  $54\text{ mm}\times 54\text{ mm}$  (outer coils), and a center-to-center spacing of  $25.5\text{ mm}$  and  $29.5\text{ mm}$ , respectively. They are tightly sandwiched between the movable quadrupole coils used for transport ( $6.0\text{ cm}$  vertical clearance), which each have an inner (outer) diameter of  $4.4\text{ cm}$  ( $11.5\text{ cm}$ ) and a height of  $4.0\text{ cm}$ . The science cell is a small quartz glass cell with inner dimensions of  $10\times 20\times 45\text{ mm}^3$  and  $1.25\text{ mm}$  wall thickness, which is fused to a glass-to-metal adapter (not shown). Also sketched are the laser beams forming the crossed optical dipole trap as described in section V.

the ohmic resistance by canceling the inductance with a matching capacitor. The measured inductance of the outer (inner) coil pair is  $190\ \mu\text{H}$  ( $110\ \mu\text{H}$ ). The PA can easily supply the ac currents for a  $60\text{ G}$  bias field directly into the resulting loads of  $\sim 1\ \Omega$ , without the need for step-up transformers. The amplitude of the ac current through each coil pair is actively stabilized to within  $\sim 10^{-4}$  using the circuit outlined in figure 3. The regulation bandwidth of about  $200\text{ Hz}$  is more than sufficient for compensating thermal drifts in the coil resistance §. The current can be switched off within less than  $1\text{ ms}$  limited by the quality factor of the matched coil pair.

#### 4. Condensate production in the McTOP trap

After transport into the science cell, the atom cloud typically contains  $1.6\times 10^9$  atoms in the  $|1, -1\rangle$  state at a phase-space density of  $5\times 10^{-7}$ . Forced radio-frequency (rf) evaporative cooling is initially performed in the stiff linear potential of the fully-compressed quadrupole trap ( $350\text{ G/cm}$  axial gradient), where it is more efficient until Majorana losses outweigh the advantage of a linear potential [21]. After a  $14\text{ s}$ -long linear rf evaporation ramp down to a temperature of  $75\ \mu\text{K}$  and an atom number of  $7\times 10^7$ , the phase-space density has increased to  $1\times 10^{-4}$  and the lifetime in the

§ An alternative, fast feedback scheme has been described in [19], where the focus is on reducing current noise to improve the coherence time for condensate interferometry in a special TOP waveguide [18].

quadrupole trap due to Majorana losses has decreased to 35 s. At this point, the trap is converted into a TOP trap by switching on an 18 G rotating bias field, which preserves the atom number to within 15% and the phase-space density to within a factor of two. The resulting harmonic trapping potential has measured trap frequencies of 70.4 Hz in the axial and 25.0 Hz in the radial direction. The trap parameters are held constant for the remaining 30 s of the evaporation sequence, during which another piecewise-linear rf ramp takes the cloud to quantum degeneracy, cf. figure 4(a).

We have found the shot-to-shot position reproducibility of the condensate to be consistent with the specified positioning uncertainty of the translation stages ( $3\sigma = 3\mu\text{m}$ ) once the system is warmed up, as shown in figure 4(b). For this measurement, the condensate was imaged simultaneously along two orthogonal axes in the horizontal  $xy$ -plane with standard resonant absorption imaging on the repump transition, immediately after the magnetic trap had turned off. We have not observed any systematic shifts of the condensate position caused by the “dual” imaging itself for the beam intensities used.

During the first 63 of a total of 173 consecutive runs after a cold start, the condensate position drifts by roughly  $15\mu\text{m}$ , as seen in figure 4(b). In the  $z$ -direction we find a similar drift of about  $7\mu\text{m}$ . This initial drift is directly correlated with the slow temperature increase and subsequent stabilization at  $\sim 75^\circ\text{C}$  of the supply cables (4/0 AWG, i.e. 11.6 mm core diameter) of the quadrupole coils. As the cables warm up, their thick rubber insulation becomes much less rigid, thus changing the mechanical torque exerted on the coil holder. This potential problem can most easily be avoided by pre-warming the cables at high quadrupole coil currents.

We have found the condensate atom number to be stable to within 5-10% depending on the performance of the MOT. For optimized conditions, condensates containing up to  $1 \times 10^6$  atoms have been observed. No correlations were found

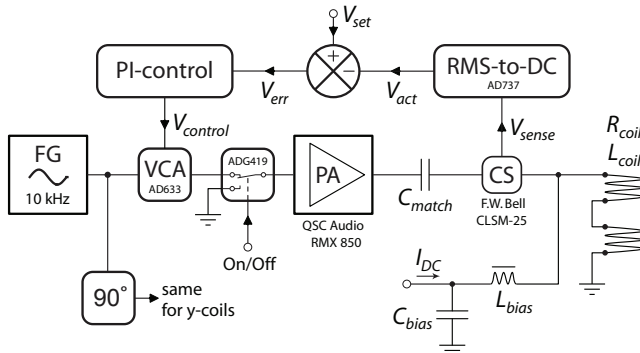


**Figure 3.** Closed-loop bias coil driving circuit (shown for one coil pair). An audio power amplifier (PA) resonantly drives the coils at 10 kHz. The coil current is sensed by a closed-loop Hall-effect current sensor (CS) whose output is converted into a dc voltage  $V_{\text{act}}$ , corresponding to the amplitude of the ac current, by an rms-to-dc converter which determines the regulation bandwidth of about 200 Hz. The error signal  $V_{\text{err}} = V_{\text{set}} - V_{\text{act}}$  is fed into an op-amp integrator that acts as a PI-controller and adjusts the gain of the voltage-controlled amplifier (VCA) to counteract any deviations from the desired amplitude  $V_{\text{set}}$ . The ac current can be switched off rapidly with an analog switch. A bias-T allows dc currents to be run through the coils independent of the ac operation, e.g. for earth-field compensation.

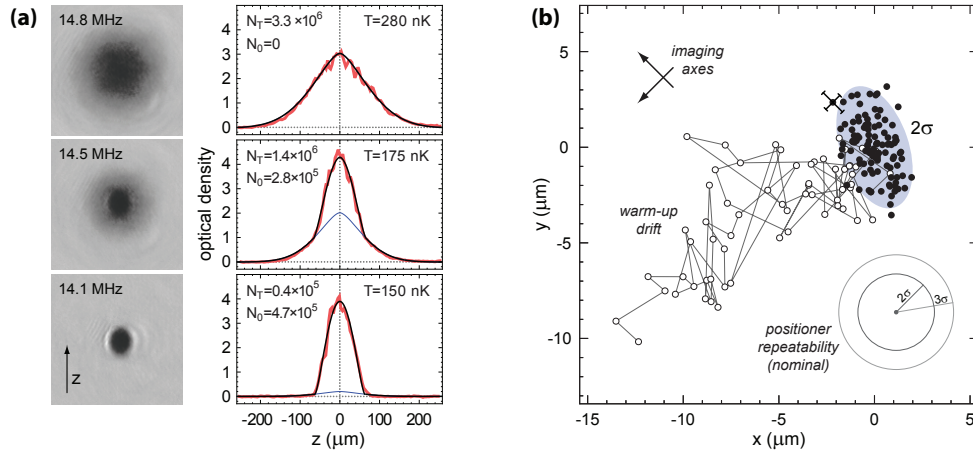


**Figure 4.** Condensate production in the McTOP trap: (a) Phase transition as seen in near-resonant absorption images after 16 ms time of flight along with vertical cuts through the density profiles. The data are fitted with the sum of two-dimensional Bose-enhanced Gaussian (thin line) and Thomas-Fermi distributions [20]. Condensation sets in at a critical temperature of  $(223 \pm 12)$  nK at which the cloud contains  $(2.7 \pm 0.4) \times 10^6$  atoms. (b) Reproducibility of the condensate position in the horizontal plane. The filled circles show the in-situ positions of the condensate (as determined from simple Gaussian fits) for the last 110 of a series of 173 runs. The  $2\sigma$  ellipsoid (shaded) with 95% of the runs has half-lengths of  $3.3 \mu\text{m}$  and  $1.8 \mu\text{m}$ , comparable to the specified repeatability of the translation stages. The open circles represent a warm-up drift during the first 63 runs (see text). The arrows indicate the two imaging directions used, and the error bars indicate the maximum uncertainty in the fits used to determine the condensate position. The radial Thomas-Fermi diameter of the trapped condensate is  $\sim 40 \mu\text{m}$ .

between the atom number and the position jitter of the cloud in the science cell.

## 5. A retractable funnel for optical trapping

For condensate production in an optical trap, the evaporation in the McTOP trap can also be used as an intermediate step after which the quadrupole coils are moved out of the way. The stationary bias-field coils can then still be used to control the spin quantization axis, for example.

The experimental procedure is as follows. After RF evaporation in the magnetic potential, the atoms are loaded adiabatically into a crossed-beam optical dipole trap formed by two orthogonally intersecting laser beams. This is done by smoothly ramping up the optical potential over 400 ms and then smoothly ramping down the magnetic confinement over another 400 ms. After the transfer, the quadrupole coils are moved back to the intermediate position ‘b’ indicated in figure 1. The Gaussian laser beams of the crossed optical dipole trap (cf. figure 2) have a  $1/e^2$  radius of  $\sim 135 \mu\text{m}$  and a combined power of 3 W. They are derived from a single-frequency 1064 nm ytterbium fiber laser (IPG YLR LP-SF series) with a relative frequency offset of 20 MHz to average out interference effects. The depth of the optical trap, including gravity, is  $6 \mu\text{K}$  in the horizontal and  $1 \mu\text{K}$  in the vertical direction. This allows for efficient gravity-assisted evaporation of atomic clouds. We typically load the optical

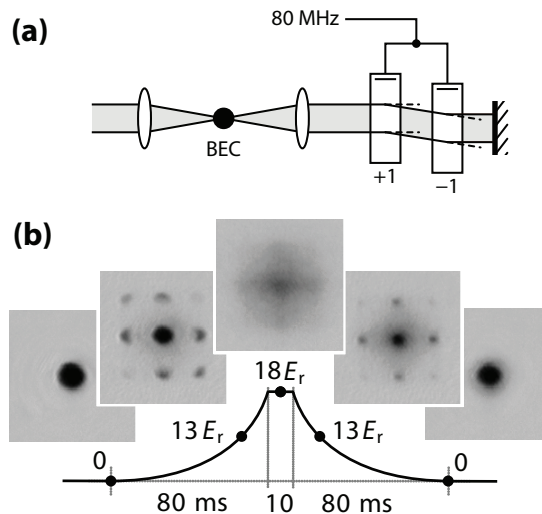


**Figure 5.** All-optical trapping and manipulation of a condensate after transfer from the McTOP trap. (a) Conversion of each of the two beams of the crossed dipole trap (cf. figure 2) into an optical lattice beam by partial retro-reflection, using a double-pass AOM configuration [22] with zero net frequency shift and rapidly adjustable reflectivity of  $10^{-6}$ - $10^{-1}$ . To realize a three-dimensional lattice, a third beam pair (with full retro-reflection) is added along  $z$ . (b) Superfluid-to-Mott insulator transition in a three-dimensional optical lattice as observed in absorption images after 18 ms time-of-flight. The lattice depth follows exponential ramps of 80 ms duration, separated by a 10 ms hold time at a depth of 18 recoil energies (solid line).

trap with clouds at  $\sim 250$  nK and then ramp down the trap depth to  $5 \mu\text{K}$  in the horizontal and 200 nK in the vertical direction where condensation sets in. At this point, the trap is nearly isotropic with measured frequencies between 50 and 60 Hz. The loading procedure results in nearly pure condensates with atom numbers that are within 90% of those reached in the McTOP trap.

By performing the final evaporation in an optical trap, it is possible to easily use the TOP trap for optical lattice experiments, thus avoiding the usual drawback of TOP traps: atomic micromotion [23] can lead to strong heating due to an oscillatory motion of the atoms relative to the lattice at the frequency of the rotating bias field [24]. To demonstrate the suitability of the approach presented in this paper, figure 5 shows data for the superfluid-to-Mott insulator transition in a three-dimensional optical lattice [25, 26] obtained with our apparatus.

## 6. Conclusion

We have demonstrated a versatile and simple scheme for producing magnetically and optically-trapped condensates in a moving-coil transporter apparatus. In our scheme, the movable quadrupole coils are also used as an essential part of the final magnetic trap. As a stand-alone device, this trap reliably produces condensates with minimal technical complexity. In experiments with optically-trapped Bose-Einstein condensates, the quadrupole coils can be retracted before quantum degeneracy is reached, providing large optical access. The apparatus is well-suited for experiments



with optical lattices, as demonstrated by observing the superfluid-to-Mott insulator transition.

## Acknowledgments

We thank R. D. Schiller, D. E. Sproles, B. Bogucki, H. Ruf, and A. Hansen for contributions in the early stages of the experiment, and R. Reimann for contributions to the optical lattice implementation. This work was funded by the Research Foundation of SUNY, the Office of Naval Research (DURIP program), and fellowships from the Fulbright program of the U.S. Department of State (S. A.) and from the GAANN program of the U.S. Department of Education (B. G.).

## References

- [1] Inouye S, Andrews M R, Stenger J, Miesner H J, Stamper-Kurn D M and Ketterle W 1998 *Nature* **392** 151
- [2] Chang M-S, Hamley C D, Barrett M D, Sauer J A, Fortier K M, Zhang W, You L and Chapman M S 2004 *Phys. Rev. Lett.* **92** 140403
- [3] Bloch I, Dalibard J and Zwirger W 2008 *Rev. Mod. Phys.* **80** 885
- [4] Barrett M D, Sauer J A and Chapman M S 2001 *Phys. Rev. Lett.* **87** 010404
- [5] Folman R, Krüger P, Schmiedmayer J, Denschlag J and Henkel C 2002 *Adv. At. Mol. Opt. Phys.* **48** 263
- [6] Greiner M, Bloch I, Hänsch T W and Esslinger T 2001 *Phys. Rev. A* **63** 031401(R)
- [7] Lewandowski H J, Harber D M, Whittaker D L and Cornell E A 2003 *J. Low Temp. Phys.* **132** 309
- [8] Gustavson T L, Chikkatur A P, Leanhardt A E, Görlitz A, Gupta S, Pritchard D E and Ketterle W 2001 *Phys. Rev. Lett.* **88** 020401
- [9] Streed E W, Chikkatur A P, Gustavson T L, Boyd M, Torii Y, Schneble D, Campbell G K, Pritchard D E and Ketterle W 2006 *Rev. Sci. Instrum.* **77** 023106
- [10] Petrich W, Anderson M H, Ensher J R and Cornell E A 1995 *Phys. Rev. Lett.* **74** 3352
- [11] Davis K B, Mewes M-O, Andrews M R, van Druten N J, Durfee D S, Kurn D M and Ketterle W 1995 *Phys. Rev. Lett.* **75** 3969
- [12] Naik D S and Raman C 2005 *Phys. Rev. A* **71** 033617
- [13] Lin Y-L, Perry A R, Compton R L, Spielman I B and Porto J V 2009 *Preprint* arXiv:0904.3314v1
- [14] Anderson B P and Kasevich M A 2001 *Phys. Rev. A* **63** 023404
- [15] Klempt C, van Zoest T, Henninger T, Topic O, Rasel E, Ertmer W and Arlt J 2006 *Phys. Rev. A* **73** 013410
- [16] Nakagawa K, Suzuki Y, Horikoshi M and Kim J B 2005 *Appl. Phys. B* **81** 791
- [17] Esslinger T, Bloch I and Hänsch T W 1998 *Phys. Rev. A* **58** 2664(R)
- [18] Reeves J M, Garcia O, Deissler B, Baranowski K L, Hughes K J and Sackett C A 2005 *Phys. Rev. A* **72** 051605(R)
- [19] Baranowski K L and Sackett C A 2006 *J. Phys. B: At. Mol. Opt. Phys.* **39** 2949
- [20] Ketterle W, Durfee D S and Stamper-Kurn D M 1999 Making, probing and understanding Bose-Einstein condensates *Proc. Int. School Phys. "Enrico Fermi" Course CXL* eds. M Inguscio and S Stringari and C E Wieman (Amsterdam: IOS Press)
- [21] Ketterle W and van Druten N J 1996 *Adv. At. Mol. Opt. Phys.* **37** 181
- [22] Gemelke N, Zhang X, Hung C-L and Chin C 2009 *Preprint* arXiv:0904.1532v1
- [23] Müller J H, Morsch O, Ciampini D, Anderlini M, Mannella R and Arimondo E 2000 *Phys. Rev. Lett.* **85** 4454
- [24] Cristiani M, Morsch O, Müller J H, Ciampini D and Arimondo E 2002 *Phys. Rev. A* **65** 063612
- [25] Jaksch D, Bruder C, Cirac J I, Gardiner C W and Zoller P 1998 *Phys. Rev. Lett.* **81** 3108
- [26] Greiner M, Mandel O, Esslinger T, Hänsch T W and Bloch I 2002 *Nature* **415** 39